

## Ab Initio and Kinetic Calculations for the Reactions of H with $(\text{CH}_3)_{(4-n)}\text{GeH}_n$ ( $n = 1, 2, 3, 4$ )

Qingzhu Zhang, Dongju Zhang, Shaokun Wang, and Yueshu Gu\*

School of Chemistry and Chemical Engineering, Shandong University, Jinan 250100, P. R. China

Received: July 16, 2001; In Final Form: September 28, 2001

The direct hydrogen abstraction reactions of H atom with  $\text{GeH}_4$ ,  $\text{CH}_3\text{GeH}_3$ ,  $(\text{CH}_3)_2\text{GeH}_2$ , and  $(\text{CH}_3)_3\text{GeH}$  have been studied systematically using ab initio molecular orbital theory. Geometries have been optimized at the UMP2 level with 6-31G(d) and 6-311G(2df,p) basis sets. G2MP2 theory has been used in the final single-point energy calculation. Theoretical analysis provided conclusive evidence that the main process occurring in each case is the hydrogen abstraction from the Ge–H bond leading to the formation of the  $\text{H}_2$  and germyl radicals; the hydrogen abstraction from the C–H bond has higher barriers and is difficult to react. The kinetic calculations of the title reactions have been deduced using the canonical variational transition-state theory (CVT) with the small-curvature tunneling correction method (SCT) over the temperature range of 200–3000 K. The CVT/SCT rate constants exhibit typical non-Arrhenius behavior. Three-parameter rate–temperature formulas have been fitted as follows:  $k_1 = (2.17 \times 10^{-17})T^{2.16} \exp(-294.2/T)$ ,  $k_2 = (2.21 \times 10^{-17})T^{2.22} \exp(-161.6/T)$ ,  $k_3 = (1.96 \times 10^{-17})T^{2.18} \exp(-108.0/T)$ , and  $k_4 = (6.66 \times 10^{-18})T^{2.33} \exp(-60.3/T)$  for the reactions of H with  $\text{GeH}_4$ ,  $\text{CH}_3\text{GeH}_3$ ,  $(\text{CH}_3)_2\text{GeH}_2$ , and  $(\text{CH}_3)_3\text{GeH}$ , respectively (in units of  $\text{cm}^3 \text{ molecule}^{-1} \text{ s}^{-1}$ ). Studies show that the methyl substitution has an effect on the strength and reactivity of the Ge–H bond in  $(\text{CH}_3)_{(4-n)}\text{GeH}_n$  ( $n = 1-3$ ). The calculated CVT/SCT rate constants are in excellent agreement with the available experimental values.

### I. Introduction

The reactions of H atom with  $\text{GeH}_4$ ,  $\text{CH}_3\text{GeH}_3$ ,  $(\text{CH}_3)_2\text{GeH}_2$ , and  $(\text{CH}_3)_3\text{GeH}$  are considered to play important roles in the chemistry of chemical vapor deposition (CVD) processes used in the semiconductor industry.<sup>1–2</sup>



Reaction A is also considered to be one of the processes that determines the abundance of  $\text{GeH}_4$  in the atmospheres of Jupiter and Saturn.<sup>3–4</sup>

For the reaction of H with  $\text{GeH}_4$ , several experimental studies were reported. The early two studies performed by Choo et al.<sup>5</sup> and Austin and Lampe<sup>6</sup> produced conflicting results. In an attempt to adjudicate between them and to extend measurements to other temperatures, Nava et al.<sup>7</sup> and Arthur and co-workers<sup>8,9</sup> studied this reaction successively, and they obtained satisfactory agreements. Arthur and co-workers measured the rate constants over the temperature range of 293–473 K and combined their results with those of Nava et al. to give a best value for rate constants of  $k_1 = (1.21 \pm 0.10) \times 10^{-10} \exp[(-1008 \pm 25)/T]$  (in  $\text{cm}^3 \text{ molecule}^{-1} \text{ s}^{-1}$ ) over the temperature range of 200–500 K. Theoretically, three investigations were reported for this reaction. In 1975, Choo and co-workers<sup>5</sup> studied this reaction

using the bond-energy bond-order (BEBO) method of Johnston,<sup>10</sup> and they found that the activation energy was overestimated with respect to the experimental data. In 1999, Espinosa-Garcia<sup>11</sup> constructed the potential energy surface of this reaction. Thermal- and vibrational-state-selected rate constants were obtained over the temperature range of 200–500 K. In 2000, Yu and co-workers<sup>12</sup> studied the reaction using ab initio molecular orbital theory combined with the canonical variational transition state theory. The geometric parameters and frequencies were calculated at the QCISD/6-311+G(d,p) level, and the energies were calculated at the G2 level of theory. The rate constants were obtained over the temperature range of 200–1600 K; a three-parameter expression was fitted:  $k_1 = (2.0 \times 10^7)T^{2.12} \exp(-492/T)$  (in  $\text{cm}^3 \text{ mol}^{-1} \text{ s}^{-1}$ ).

However, for the reactions of H with  $\text{CH}_3\text{GeH}_3$ ,  $(\text{CH}_3)_2\text{GeH}_2$ , and  $(\text{CH}_3)_3\text{GeH}$ , the situations have been poorer still. Only two groups<sup>13–15</sup> studied experimentally these reactions. In 1977, Austin and Lampe<sup>13</sup> measured their rate constants using an indirect method. In 1998, Arthur and Miles<sup>14</sup> obtained their Arrhenius expressions using a direct method:  $k_4 = (8.80 \pm 1.09) \times 10^{-11} \exp[(-929 \pm 45)/T]$  for H with  $(\text{CH}_3)_3\text{GeH}$ ,  $k_3 = (9.64 \pm 1.51) \times 10^{-11} \exp[(-854 \pm 56)/T]$  for H with  $(\text{CH}_3)_2\text{GeH}_2$  (in  $\text{cm}^3 \text{ molecule}^{-1} \text{ s}^{-1}$ ); for the reaction of H with  $\text{CH}_3\text{GeH}_3$ , only one rate constant<sup>15</sup> was obtained (298 K) and the value is  $k_2 = (4.97 \pm 0.27) \times 10^{-12}$  (in  $\text{cm}^3 \text{ molecule}^{-1} \text{ s}^{-1}$ ) at 298 K. To our knowledge, little theoretical attention has been paid to the reactions of H with methylgermanes.

We have initiated a systematic and theoretical study of the application of ab initio electronic calculations combined with the variational transition-state theory for the reactions of atomic H with  $(\text{CH}_3)_{(4-n)}\text{GeH}_n$  ( $n = 1-4$ ). The reasons for initiating such a work are threefold. First, the reaction mechanisms and

\* To whom correspondence should be addressed. E-mail: guojz@icm.sdu.edu.cn.

kinetic nature of these reactions are essential input data for computer-modeling studies directed toward obtaining an understanding of the factors controlling CVD processes. Second, Si and Ge belong to the same group. A number of investigations of the effect of methyl substitution on the reactivity of the Si–H bond in  $\text{SiH}_4$  toward attack by various radicals have been reported.<sup>16–21</sup> In the case of H atom attack, a clear trend is evident: the reactivity of the Si–H bond, as measured by the room-temperature rate constant corrected for reaction path degeneracy,  $k/n$ , increases smoothly from  $\text{SiH}_4$  to  $(\text{CH}_3)_3\text{SiH}$ .<sup>20–21</sup> However, much less is known concerning the reactivity of the Ge–H bond in  $\text{GeH}_4$ . Only two studies are on record: Austin and Lampe<sup>13</sup> and Arthur and Miles<sup>15</sup> concluded from their experimental studies that successive methyl substitution enhances the reactivity of the Ge–H bond. Their conclusion needs a theoretical support. Third, it is well-known that there is a significant computational difficulty in treating relatively large electronic systems containing several heavier atoms. The theory level of QCISD/6-311+G(d,p), which Yu et al.<sup>12</sup> used in the study of the reaction of H with  $\text{GeH}_4$ , is much higher, and the results that Yu obtained are very reliable. However, it is much more expensive for the reactions of H with methylgermanes, especially for the reaction of H with  $(\text{CH}_3)_3\text{GeH}$  (it need greater computational condition). In this paper, we have used the reliable experimental and theoretical data of the reaction of H with  $\text{GeH}_4$  to make a serious test of the applicability of the current quantum chemistry methodologies. The purpose is to find a viable theory level that should be inexpensive but adequate for the reactions of H with methylgermanes, especially for H with  $(\text{CH}_3)_3\text{GeH}$ .

Several important features of this study are as follows: (1) The reaction mechanism has been revealed. (2) The rate constants have been obtained using canonical variational transition-state theory with small-curvature tunneling effect (CVT/SCT) over a wide temperature range of 200–3000 K. (3) The non-Arrhenius expression has been fitted. (4) The results of CVT/SCT calculations are compared with experimental values and other theoretical results. (5) The effect of methyl substitution on the strength and reactivity of the Ge–H bond has been discussed.

## II. Computation Methods and Theory

Ab initio calculations have been carried out using Gaussian 94 programs.<sup>22</sup> The geometries of reactants, transition states, and products have been optimized at the UMP2(FULL) level with 6-31G(d). To check the dependence of the ab initio results on the basis sets, a more flexible basis set, 6-311G(2df,p), has been used to optimize the geometry of the transition states (computationally more expensive). The vibrational frequencies have been calculated at the UMP2(FULL)/6-31G(d) level to determine the nature of different stationary points and the zero-point energy (ZPE) (scaled by a factor of 0.95). The number of imaginary frequencies (0 or 1) confirms whether a bound minimum or a transition state has been located. The intrinsic reaction coordinate (IRC) calculation confirms that the transition state connects the designated reactants and products. At the UMP2(FULL)/6-31G(d) level, the minimum energy path (MEP) has been obtained with a gradient step size of 0.05 amu<sup>1/2</sup> b in mass-weighted Cartesian coordinates for each reaction. The force constant matrixes of the stationary and selected nonstationary points near the transition state along the MEP have also been calculated for each reaction. Because the shape of the MEP is important for the calculation of the rate constants, the single-point energies have been calculated at the MP2, QCISD(T), and

G2MP2 levels for the reaction of H with  $\text{GeH}_4$ . The larger basis, 6-311++G(3df,3pd), has been used in these calculations. The G2MP2 has been used for the energy calculation of the reactions of H with methylgermanes. All relative energies quoted and discussed in the present paper include zero-point energy corrections with scaled vibrational frequencies.

The initial information obtained from our ab initio calculations allowed us to calculate the variational rate constants including the tunneling effects. The canonical variational theory (CVT)<sup>23–25</sup> rate constant for temperature  $T$  is given by

$$k^{\text{CVT}}(T) = \min_s k^{\text{GT}}(T,s) \quad (1)$$

where

$$k^{\text{GT}}(T,s) = \frac{\sigma k_{\text{B}} T}{h} \frac{Q^{\text{GT}}(T,s)}{\Phi^{\text{R}}(T)} e^{-V_{\text{MEP}}(s)/(k_{\text{B}} T)} \quad (2)$$

where,  $k^{\text{GT}}(T,s)$  is the generalized transition state theory rate constant at the dividing surface,  $s$ ,  $\sigma$  is the symmetry factor accounting for the possibility of more than one symmetry-related reaction path,  $k_{\text{B}}$  is Boltzmann's constant,  $h$  is Planck's constant,  $\Phi^{\text{R}}(T)$  is the reactant partition function per unit volume, excluding symmetry numbers for rotation, and  $Q^{\text{GT}}(T,s)$  is the partition function of a generalized transition state at  $s$  with a local zero of energy at  $V_{\text{MEP}}(s)$  and with all rotational symmetry numbers set to unity. The tunneling correction has been considered by using the centrifugal-dominant small-curvature semiclassical adiabatic ground-state (CD-SCSAG) method. All the kinetic calculations have been carried out using the POLYRATE 7.8 program.<sup>26</sup>

## III. Result and Discussion

The optimized geometries of reactants, transition states, and products are shown in Figure 1. The transition state of the reaction of H with  $\text{GeH}_4$  is denoted as  $\text{TS}_1$ , while the transition states of the reactions of H with  $\text{CH}_3\text{GeH}_3$ ,  $(\text{CH}_3)_2\text{GeH}_2$ , and  $(\text{CH}_3)_3\text{GeH}$  are denoted as  $\text{TS}_2$ ,  $\text{TS}_3$  and  $\text{TS}_4$ . The vibrational frequencies of reactants and products are listed in Table 1, and the frequencies of the transition states are listed in Table 2. The potential barrier,  $\Delta E$ , and the reaction enthalpy,  $\Delta H$ , calculated are summarized in Table 3 for the reaction of H with  $\text{GeH}_4$  and in Table 4 for the reactions of H with methylgermanes. The calculated CVT/SCT rate constants are presented in Table 5 and the experimental values are depicted in Table 6.

**1. The Reaction Mechanism.** It is worth stating the reliability of the calculations in this work. Because unrestricted Hartree–Fock (UHF) reference wave functions are not spin eigenfunctions for open-shell species, we monitored the expectation values of  $\langle S^2 \rangle$  in the UMP2 optimization. The  $\langle S^2 \rangle$  values are always in the range of 0.750–0.778 for doublets at the UMP2(FULL)/6-31G(d) level. After spin annihilation, the values of  $\langle S^2 \rangle$  are 0.750, where 0.750 is the exact value for a pure doublet. Thus, spin contamination is not severe in the UMP2 optimization for the title reactions. This suggests that a single-determinant reference wave function for this system is suitable for the level of theory used in the optimization.<sup>27</sup>

To clarify the general reliability of the theoretical calculations, it is useful to compare the predicted chemical properties of the present particular systems of interest with experimental data. As shown in Figure 1, the calculated geometric parameters of  $\text{GeH}_4$ ,  $\text{CH}_3\text{GeH}_3$ ,  $(\text{CH}_3)_2\text{GeH}_2$ , and  $(\text{CH}_3)_3\text{GeH}$  are in good agreement with the available experimental values. From this result, it might be inferred that the same accuracy could be

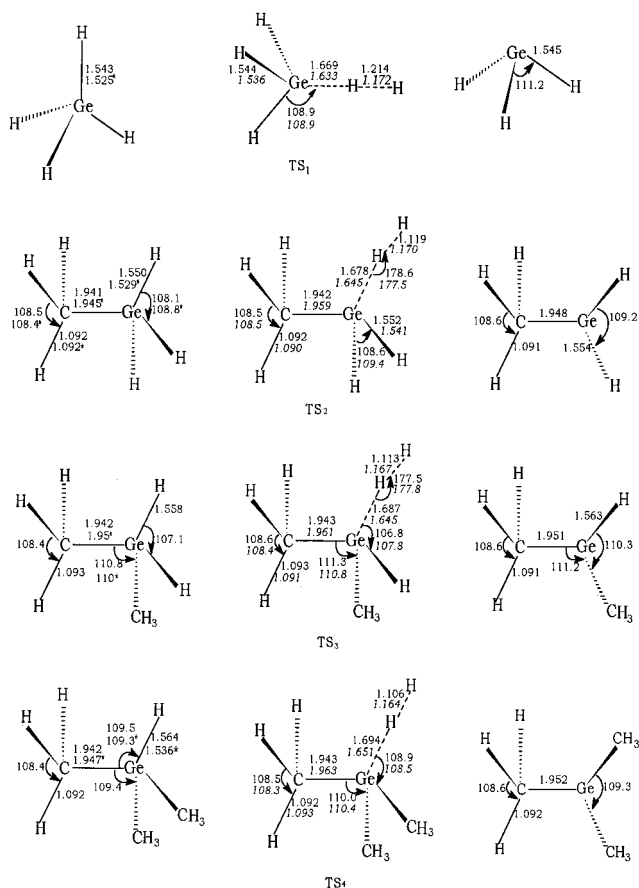


**Figure 1.** The optimized geometries for reactants, transition states, and products at UMP2(FULL)/6-31G(d) level. The values with asterisks are the experimental data.<sup>28,42</sup> The values in italics are calculated at UMP2/6-311G(2df,p) level. The bond length is in Å, and the bond angle is in deg.

expected for the calculated geometry parameters of the transition states. To check the dependence of the ab initio results on the basis set, we performed the UMP2 calculation with the flexible 6-311G(2df,p) basis set (computationally more expensive) for the transition states. The optimized geometrical parameters are also shown in Figure 1. Compared with the results calculated at UMP2(FULL)/6-31G(d), it can be seen that extension of the basis set, 6-311G(2df,p), does not cause observable change. As can be seen from Table 1, the scaled vibrational frequencies of the reactants agree well with the experimentally observed fundamentals, and the maximum relative error is 8%. These good agreements give us confidence that the UMP2(FULL)/6-31G(d) theory level is adequate to optimize the geometries and to calculate the frequencies.

*a. The H with GeH<sub>4</sub> Reaction.* The reaction of H with GeH<sub>4</sub> had always been studied theoretically at much higher level.<sup>11–12</sup> We have studied this reaction for two purposes: (1) comparison with the reactions of H with methylgermanes and (2) testing the reliability of our calculations.

The reaction of H with GeH<sub>4</sub> proceeds via a direct abstraction mechanism. For the transition state TS<sub>1</sub> of this reaction, at the UMP2(FULL)/6-31G(d) level, the forming H–H bond of 1.214 Å is 64.49% longer than the equilibrium value of 0.738 Å in H<sub>2</sub>, while the breaking Ge–H bond is stretched by 8.17%. The transition states are reactant-like. Therefore, this reaction will proceed via an early transition state. This rather early character in the transition state is in accordance with the low reaction barrier and the high exothermicity of this reaction, in keeping with Hammond's postulate. TS<sub>1</sub> has a large imaginary fre-

quency, which implies that the quantum tunneling effect may be significant and may play an important role in the calculation of the rate constants. TS<sub>1</sub> has C<sub>3v</sub> symmetry.

Table 3 lists the potential barriers ( $\Delta E$ ) and the reaction enthalpies ( $\Delta H$ ), computed at different levels of theory and taking into account the zero-point energy differences, for the reaction of H with GeH<sub>4</sub>. First, we analyze the reaction enthalpy. Espinosa-Garcia<sup>11</sup> obtained a better experimental value of  $-21.21$  kcal/mol from the measured  $\Delta H_{f,0}$  for GeH<sub>4</sub>, GeH<sub>3</sub>, and H. The value of  $-17.39$  kcal/mol calculated at the MP2 level with 6-311+G(3df,2p) is in great disagreement with the experimental value ( $-21.21$  kcal/mol); a similar calculation using the same basis set with the highly correlated and more computationally demanding QCISD(T) level predicts the value of  $-19.49$  kcal/mol, in excellent agreement with the experimental value. These results clearly indicated that most of the error in the reaction enthalpy computed at MP2 with the 6-311+G(3df,2p) basis set can be attributed to the lack of correlation in such a method and not to an improper optimized geometry at UMP2/6-31G(d). Results obtained at G2MP2 and QCISD(T)/6-311++G(3df,3pd) are in good agreement with the experimental value, especially if the experimental uncertainty for GeH<sub>3</sub> ( $\pm 2$  kcal/mol) is taken into consideration.

It can be seen from Table 3 that the potential barrier has a great discrepancy obtained at different levels. The values calculated at the UMP2 level with different basis sets are much greater than those obtained at the highly correlated and more computationally demanding QCISD(T) level. The value calculated at the QCISD(T)/6-311G(d,p) level is greater about 1 kcal/mol than that calculated at the QCISD(T)/6-311+G(3df,2p) level; this means that the size of the basis set will have an important effect on the potential barrier calculated. The value calculated at G2MP2 level is in good agreement with the values calculated at the QCISD(T)/6-311+G(3df,2p) and QCISD(T)/6-311++G(3df,3pd) levels, while the computational time and demanding of the G2MP2 level are much less than those of the QCISD(T)/6-311+G(3df,2p) and QCISD(T)/6-311++G(3df,3pd) levels. This means that G2MP2 is a good choice to compute the potential barrier. It also can be seen that the value calculated at G2MP2//UMP2(FULL)/6-31G(d) is very close to the value obtained at G2MP2//UMP2/6-311G(2df,p).

The objective of the study of the reaction of H with GeH<sub>4</sub> is to develop an inexpensive method that can be applied to methylgermanes, especially to (CH<sub>3</sub>)<sub>3</sub>GeH. Thus, although the QCISD(T)/6-311+G(3df,2p) and QCISD(T)/6-311++G(3df,3pd) levels result in better values of the potential barriers, they are too computationally intensive to be generally applicable for the reaction of H with methylgermanes at the present time. Therefore, in this work, we have chosen the energies computed at G2MP2//UMP2(FULL)/6-31G(d) to calculate the reaction rate constants. These rate constants are determined as a function of temperature and potential barrier calculated from this dependence.

*b. Reactions of H with (CH<sub>3</sub>)<sub>(4-n)</sub>GeH<sub>n</sub> (n = 1–3).* As mentioned above, the reactions of H with CH<sub>3</sub>GeH<sub>3</sub>, (CH<sub>3</sub>)<sub>2</sub>GeH<sub>2</sub>, and (CH<sub>3</sub>)<sub>3</sub>GeH can react through two channels: the hydrogen abstraction from the Ge–H bond and the hydrogen abstraction from the C–H bond. A good approximation for the rate constants attack on the methyl groups can be obtained by considering the rate constants of the reactions of H with (CH<sub>3</sub>)<sub>4</sub>Si and (CH<sub>3</sub>)<sub>4</sub>Ge. At 305 K, Austin and Lampe found both reactions to be too slow to measure, but a rate constant can be evaluated from the Arrhenius parameters for (CH<sub>3</sub>)<sub>4</sub>Si reported by Potzinger.<sup>33</sup> The value at 298 K is  $1.15 \times 10^{-16}$  cm<sup>3</sup>



**TABLE 1: The Frequencies (Scaled by 0.95, in cm<sup>-1</sup>) of Reactants and Products Involved in the Reactions of H with (CH<sub>3</sub>)<sub>(4-n)</sub>GeH<sub>n</sub> (n = 1–4) at UMP2(FULL)/6-31G(d)<sup>a</sup>**

species	frequencies													
GeH <sub>4</sub>	834	834	834	946	946	2120	2142	2142	2142					
	<i>819</i>	<i>819</i>	<i>819</i>	<i>913</i>	<i>913</i>	<i>2106</i>	<i>2114</i>	<i>2114</i>	<i>2114</i>					
CH <sub>3</sub> GeH <sub>3</sub>	170	498	498	612	811	842	842	884	884	1291	1460	1460	1460	
	2086	2102	2102	2968	3063	3063								
	<i>157</i>	<i>506</i>	<i>506</i>	<i>602</i>	<i>843</i>	<i>848</i>	<i>848</i>	<i>900</i>	<i>900</i>	<i>1254</i>	<i>1428</i>	<i>1428</i>	<i>1428</i>	
	<i>2084</i>	<i>2085</i>	<i>2085</i>	<i>2938</i>	<i>2997</i>	<i>2997</i>								
(CH <sub>3</sub> ) <sub>2</sub> GeH <sub>2</sub>	135	154	169	398	565	597	613	642	837	849	855	868	871	1285
	1291	1455	1460	1463	1469	1948	1957	2961	2962	3054	3054			
	3059	3059												
	<i>2971</i>	<i>2061</i>												
(CH <sub>3</sub> ) <sub>3</sub> GeH	131	169	169	174	183	183	614	627	627	657	657	762	890	890
	896	906	906	1351	1351	1358	1534	1534	1536	1548	1548	1551		
	2015	3111	3111	3111	3208	3208	3209	3215	3216	3216				
	<i>187</i>	<i>592</i>	<i>850</i>	<i>833</i>	<i>624</i>	<i>1246</i>	<i>1426</i>	<i>1426</i>	<i>2922</i>	<i>2982</i>	<i>2982</i>			
GeH <sub>3</sub>	705	877	877	2085	2128	2128								
CH <sub>3</sub> GeH <sub>2</sub>	158	483	521	599	809	845	865	1281	1454	1456	1950	1977		
	2962	3054	3069											
(CH <sub>3</sub> ) <sub>2</sub> GeH	120	136	163	449	580	590	610	734	844	851	865	1274	1282	
	1452	1455	1456	1465	1917	2955	2955	3046	3046	3065	3065			
(CH <sub>3</sub> ) <sub>3</sub> Ge	114	148	148	162	170	170	563	604	604	726	726	727	851	860
	860	1271	1271	1281	1454	1454	1464	1464	1472	2947	2948			
	2948	3062	3062	3062										

<sup>a</sup> The values in italics are the experimental data from refs 29–32 and 43.

**TABLE 2: The Frequencies (Scaled by 0.95, in cm<sup>-1</sup>) of Transition States Involved in the Reactions of H with (CH<sub>3</sub>)<sub>(4-n)</sub>GeH<sub>n</sub> (n = 1–4) at UMP2(FULL)/6-31G(d)**

species	frequencies													
TS <sub>1</sub>	1708i	338	338	751	840	840	977	977	1021	1996	2131	2131		
TS <sub>2</sub>	1668i	136	185	316	510	571	609	826	848	865	964	979	1005	
	1288	1457	1458	1965	1985	2965	3058	3066						
TS <sub>3</sub>	1628i	122	141	165	178	188	518	591	592	621	732	848	853	
	964	961	965	1002	1283	1289	1454	1458	1460	1467	1933			
	2959	2959	3050	3050	3060	3060								
TS <sub>4</sub>	1581i	106	144	144	161	169	169	184	184	577	617	617	727	
	732	732	850	860	860	972	978	978	1282	1282	1289	1455		
	1455	1457	2953	2954	2954	3044	3044	3045	3058	3058	3059			

**TABLE 3: The Potential Barrier, ΔE (in kcal/mol), and the Reaction Enthalpy, ΔH (in kcal/mol), Calculated for the Reaction of H with GeH<sub>4</sub> at Various Theory Levels on the Basis of the UMP2(FULL)/6-31G(d) Geometrical Parameters and ZPE Corrections**

theory level	ΔE	ΔH
MP2/6-311G(d)	6.86	-16.95
MP2/6-311+G(3df,2p)	5.84	-17.39
QCISD(T)/6-311G(d,p)	3.99	-19.25
QCISD(T)/6-311+G(3df,2p)	2.94	-19.49
QCISD(T)/6-311++G(3df,3pd)	2.42	-20.06
G2MP2	2.96	-19.69
G2MP2 <sup>a</sup>	3.55	-19.69
	2.53 <sup>b</sup>	-21.41 <sup>b</sup>
	3.54 <sup>c</sup>	-19.22 <sup>c</sup>
exptl		-21.21

<sup>a</sup> The values were calculated on the basis of the UMP2(FULL)/6-311G(2df,p) geometrical parameters and UMP2(FULL)/6-31G(d) ZPE corrections. <sup>b</sup> The values were obtained from potential energy surface, ref 11. <sup>c</sup> The values were done at G2//QCISD/6-311+G(d,p), ref 12.

molecule<sup>-1</sup> s<sup>-1</sup>. Adjusting for the number of C–H bond in the different germanes, Arthur and Miles evaluated that the rate constants of attack on the C–H bond are all less than 0.002% of the respective experimental rate constants<sup>15</sup> for the reactions of H with methylgermanes. The barrier heights calculated at G2MP2 level for the hydrogen abstraction from the Ge–H bond of CH<sub>3</sub>GeH<sub>3</sub>, (CH<sub>3</sub>)<sub>2</sub>GeH<sub>2</sub>, and (CH<sub>3</sub>)<sub>3</sub>GeH are 2.64, 2.38, and 2.21 kcal/mol, respectively, while the barrier heights of the hydrogen abstraction from the C–H bond are 12.51, 9.93, and

**TABLE 4: The Potential Barrier, ΔE (in kcal/mol), and Reaction Enthalpy, ΔH (in kcal/mol), calculated for the reactions of H with methylgermanes calculated at the G2MP2//UMP2(FULL)/6-31G(d) level**

reactions	ΔE	ΔH
H + CH <sub>3</sub> GeH <sub>3</sub>	2.64	-19.01
H + (CH <sub>3</sub> ) <sub>2</sub> GeH <sub>2</sub>	2.38	-18.33
H + (CH <sub>3</sub> ) <sub>3</sub> GeH	2.21	-17.82

11.74 kcal/mol, respectively, which are much higher than that of the hydrogen abstraction from the Ge–H bond. Thus, we can safely say that attack on the methyl groups in the methylgermanes is negligible, which is similar to the mechanism of the reactions of H with CH<sub>3</sub>SiH<sub>3</sub>, (CH<sub>3</sub>)<sub>2</sub>SiH<sub>2</sub>, and (CH<sub>3</sub>)<sub>3</sub>SiH.<sup>34</sup> Therefore, we mainly discuss the hydrogen abstraction reactions from the Ge–H bond.

The transition states of the hydrogen abstractions from Ge–H bond of CH<sub>3</sub>GeH<sub>3</sub>, (CH<sub>3</sub>)<sub>2</sub>GeH<sub>2</sub>, and (CH<sub>3</sub>)<sub>3</sub>GeH are denoted as TS<sub>2</sub>, TS<sub>3</sub>, and TS<sub>4</sub>, respectively. Their geometrical parameters calculated at the UMP2/6-31G(d) level are shown in Figure 1. For the reactions of H with CH<sub>3</sub>GeH<sub>3</sub> and (CH<sub>3</sub>)<sub>2</sub>GeH<sub>2</sub>, the H atom attacks one H of Ge–H bonds with a slightly bent orientation angle of 178.6° and 177.8°, respectively. Thus, the transition states, TS<sub>2</sub> and TS<sub>3</sub>, have C<sub>s</sub> symmetry. For the reaction of H with (CH<sub>3</sub>)<sub>3</sub>GeH, the H atom attacks linearly the H of the Ge–H bond, and the transition state TS<sub>4</sub> has C<sub>3v</sub> symmetry. For the transition states TS<sub>2</sub>, TS<sub>3</sub>, and TS<sub>4</sub>, the breaking Ge–H bonds are elongated by 8.25%, 8.28%, and 8.31%, while the forming H–H bonds are longer than the equilibrium value of 0.738 Å in H<sub>2</sub> by 51.63%, 50.81%, and

**TABLE 5: The Calculated CVT/SCT Rate Constants (in  $\text{cm}^3 \text{molecule}^{-1} \text{s}^{-1}$ ) for the Reactions of H with  $\text{GeH}_4$ ,  $\text{CH}_3\text{GeH}_3$ ,  $(\text{CH}_3)_2\text{GeH}_2$ , and  $(\text{CH}_3)_3\text{GeH}$** 

<i>T</i> (K)	$\text{GeH}_4$	$\text{CH}_3\text{GeH}_3$	$(\text{CH}_3)_2\text{GeH}_2$	$(\text{CH}_3)_3\text{GeH}$
200	$5.33 \times 10^{-13}$	$1.26 \times 10^{-12}$	$1.19 \times 10^{-12}$	$1.29 \times 10^{-12}$
250	$9.51 \times 10^{-13}$	$2.44 \times 10^{-12}$	$2.15 \times 10^{-12}$	$2.02 \times 10^{-12}$
298	$1.88 \times 10^{-12}$	$4.00 \times 10^{-12}$	$3.38 \times 10^{-12}$	$3.01 \times 10^{-12}$
300	$1.63 \times 10^{-12}$	$4.07 \times 10^{-12}$	$3.44 \times 10^{-12}$	$3.07 \times 10^{-12}$
350	$2.62 \times 10^{-12}$	$6.19 \times 10^{-12}$	$5.06 \times 10^{-12}$	$4.45 \times 10^{-12}$
400	$3.94 \times 10^{-12}$	$8.82 \times 10^{-12}$	$7.04 \times 10^{-12}$	$6.24 \times 10^{-12}$
450	$5.63 \times 10^{-12}$	$1.20 \times 10^{-11}$	$9.38 \times 10^{-12}$	$8.47 \times 10^{-12}$
500	$7.71 \times 10^{-12}$	$1.57 \times 10^{-11}$	$1.21 \times 10^{-11}$	$1.11 \times 10^{-11}$
600	$1.30 \times 10^{-11}$	$2.48 \times 10^{-11}$	$1.86 \times 10^{-11}$	$1.78 \times 10^{-11}$
700	$2.00 \times 10^{-11}$	$3.63 \times 10^{-11}$	$2.68 \times 10^{-11}$	$2.65 \times 10^{-11}$
800	$2.86 \times 10^{-11}$	$5.03 \times 10^{-11}$	$3.65 \times 10^{-11}$	$3.73 \times 10^{-11}$
900	$3.89 \times 10^{-11}$	$6.68 \times 10^{-11}$	$4.79 \times 10^{-11}$	$5.02 \times 10^{-11}$
1000	$5.07 \times 10^{-11}$	$8.59 \times 10^{-11}$	$6.10 \times 10^{-11}$	$6.52 \times 10^{-11}$
1200	$7.92 \times 10^{-11}$	$1.32 \times 10^{-10}$	$9.24 \times 10^{-11}$	$1.01 \times 10^{-10}$
1400	$1.13 \times 10^{-10}$	$1.90 \times 10^{-10}$	$1.31 \times 10^{-10}$	$1.45 \times 10^{-10}$
1600	$1.54 \times 10^{-10}$	$2.59 \times 10^{-10}$	$1.77 \times 10^{-10}$	$1.98 \times 10^{-10}$
1800	$1.99 \times 10^{-10}$	$3.40 \times 10^{-10}$	$2.31 \times 10^{-10}$	$2.58 \times 10^{-10}$
2000	$2.50 \times 10^{-10}$	$4.34 \times 10^{-10}$	$2.92 \times 10^{-10}$	$3.25 \times 10^{-10}$
2200	$3.06 \times 10^{-10}$	$5.40 \times 10^{-10}$	$3.61 \times 10^{-10}$	$3.99 \times 10^{-10}$
2400	$3.66 \times 10^{-10}$	$6.60 \times 10^{-10}$	$4.38 \times 10^{-10}$	$4.81 \times 10^{-10}$
2600	$4.30 \times 10^{-10}$	$7.92 \times 10^{-10}$	$5.23 \times 10^{-10}$	$5.69 \times 10^{-10}$
2800	$4.99 \times 10^{-10}$	$9.38 \times 10^{-10}$	$6.17 \times 10^{-10}$	$6.64 \times 10^{-10}$
3000	$5.72 \times 10^{-10}$	$1.10 \times 10^{-9}$	$7.19 \times 10^{-10}$	$7.67 \times 10^{-10}$

**TABLE 6: The Experimental Rate Constants (in  $\text{cm}^3 \text{molecule}^{-1} \text{s}^{-1}$ ) for the Reactions of H with  $\text{GeH}_4$ ,  $\text{CH}_3\text{GeH}_3$ ,  $(\text{CH}_3)_2\text{GeH}_2$ , and  $(\text{CH}_3)_3\text{GeH}$** 

<i>T</i> (K)	$\text{GeH}_4^a$	$\text{CH}_3\text{GeH}_3^b$	$(\text{CH}_3)_2\text{GeH}_2^c$	$(\text{CH}_3)_3\text{GeH}^d$
200	$7.83 \times 10^{-13}$			
250	$2.14 \times 10^{-12}$			
298	$4.11 \times 10^{-12}$	$4.97 \times 10^{-12}$	$5.49 \times 10^{-12}$	$3.90 \times 10^{-12}$
300	$4.20 \times 10^{-12}$		$5.59 \times 10^{-12}$	$3.98 \times 10^{-12}$
350	$6.80 \times 10^{-12}$		$8.40 \times 10^{-12}$	$6.19 \times 10^{-12}$
400	$9.73 \times 10^{-12}$		$1.14 \times 10^{-11}$	$8.63 \times 10^{-12}$
450	$1.29 \times 10^{-11}$		$1.45 \times 10^{-11}$	$1.12 \times 10^{-11}$
500	$1.61 \times 10^{-11}$		$1.75 \times 10^{-11}$	$1.51 \times 10^{-11}$

<sup>a</sup> From ref 8:  $k_1 = (1.21 \pm 0.10) \times 10^{-10} \exp[(-1008 \pm 25)/T]$ .

<sup>b</sup> From ref 15. <sup>c</sup> From ref 14:  $k_3 = (9.64 \pm 1.51) \times 10^{-11} \exp[(-854 \pm 56)/T]$ . <sup>d</sup> From ref 14:  $k_4 = (8.80 \pm 1.09) \times 10^{-11} \exp[(-929 \pm 45)/T]$ .

49.86%, respectively. Therefore,  $\text{TS}_2$ ,  $\text{TS}_3$ , and  $\text{TS}_4$  are reactant-like, and the hydrogen abstraction reactions from  $\text{CH}_3\text{GeH}_3$ ,  $(\text{CH}_3)_2\text{GeH}_2$ , and  $(\text{CH}_3)_3\text{GeH}$  proceed via early transition states. This rather early character in these transition states is in accordance with the high exothermicities of the title reactions. It is interesting that the breaking Ge–H bond lengths are in the order of  $\text{TS}_4 > \text{TS}_3 > \text{TS}_2 > \text{TS}_1$ . However, the forming H–H bond distances have the reverse order. The type of changing trend of bond distances not only reveals the effect of methyl substitution but also reflects the sequence of energy barriers.

Table 2 shows that transition states of the hydrogen abstraction from the Ge–H bonds have one and only one imaginary frequency. The values of the imaginary frequencies are large, which implies that the quantum tunneling effect may be significant and may play an important role in the calculations of the rate constants. Table 4 shows that the three reactions of H with methylgermanes are exothermic in nature.

It is worth discussing the effect of methyl substitution on the geometrical parameters and on the reaction mechanism for the reactions of H with  $(\text{CH}_3)_{(4-n)}\text{GeH}_n$  ( $n = 1-4$ ). There are three features for the four reactions. First, the Ge–H bond length in  $\text{GeH}_4$  is 1.543 Å at UMP2(FULL)/6-31G(d) level, while the Ge–H bond lengths are 1.550, 1.558, and 1.564 Å in  $\text{CH}_3\text{GeH}_3$ ,  $(\text{CH}_3)_2\text{GeH}_2$ , and  $(\text{CH}_3)_3\text{GeH}$ . It can be seen that the Ge–H bond lengths in methylgermanes are longer than that in  $\text{GeH}_4$ ,

and the Ge–H bond length increases with the increase in methyl substitution from  $\text{CH}_3\text{GeH}_3$  to  $(\text{CH}_3)_3\text{GeH}$  through  $(\text{CH}_3)_2\text{GeH}_2$ . Second, the potential barrier of the reaction of H with  $\text{GeH}_4$  is 2.96 kcal/mol at G2MP2 level, while the potential barriers of the reactions of H with  $\text{CH}_3\text{GeH}_3$ ,  $(\text{CH}_3)_2\text{GeH}_2$ , and  $(\text{CH}_3)_3\text{GeH}$  are 2.64, 2.38, and 2.21 kcal/mol, respectively. The reaction of H with  $\text{GeH}_4$  possesses the highest potential barrier. The potential barriers of the reactions of H with methylgermanes are 0.32–0.75 kcal/mol lower than that of the H with  $\text{GeH}_4$  reaction. The more methyl substitutions the compound has; the lower barrier the reactions will have. This means that hydrogen abstraction from methylgermanes is easier than that from  $\text{GeH}_4$ . The following study of the rate constants further testifies to this view. Third, the reaction enthalpy of the reaction of H with  $\text{GeH}_4$  is  $-19.69$  kcal/mol at G2MP2, and the reaction enthalpies of the reactions of H with  $\text{CH}_3\text{GeH}_3$ ,  $(\text{CH}_3)_2\text{GeH}_2$ , and  $(\text{CH}_3)_3\text{GeH}$  are  $-19.01$ ,  $-18.33$ , and  $-17.82$  kcal/mol. It can be seen that the exothermicities of the reactions of H with methylgermanes are less than that of H with  $\text{GeH}_4$ , and the exothermicity decreases with the increase in methyl substitution from  $\text{CH}_3\text{GeH}_3$  to  $(\text{CH}_3)_3\text{GeH}$  through  $(\text{CH}_3)_2\text{GeH}_2$ . These changing trends not only reveal the effect of the methyl substitution but also reflect the sequence of the  $k/n$  value, the rate constant corrected for reaction path degeneracy. The following study of the rate constants further testifies this view.

**2. The Kinetic Calculation.** *a. Reaction Path Properties.* With a step size of 0.05  $\text{amu}^{1/2} \text{b}$ , the intrinsic reaction coordinate (IRC) has been calculated at the UMP2(FULL)/6-31G(d) level from the transition state to the reactants and the products for the title reactions. For the reaction of H with  $\text{CH}_3\text{GeH}_3$ , the breaking Ge–H bond is almost unchanged from  $s = -\infty$  to  $s = -0.5 \text{amu}^{1/2} \text{b}$  and equals the value of the reactant and stretches linearly after  $s = -0.5 \text{amu}^{1/2} \text{b}$ . The forming H–H bond shortens rapidly from reactants and reaches the equilibrium bond length of  $\text{H}_2$  at  $s = 0.5 \text{amu}^{1/2} \text{b}$ . Other bond lengths are almost unchanged during the reaction process. Therefore, the transition state  $\text{TS}_2$  connects the reactants ( $\text{CH}_3\text{GeH}_3$  and H) with the products ( $\text{CH}_3\text{GeH}_2$  and  $\text{H}_2$ ). The geometric change mainly takes place in the region from  $s = -0.5$  to  $s = 0.5 \text{amu}^{1/2} \text{b}$ . The same conclusion can be drawn from the reactions of H with  $\text{GeH}_4$ ,  $(\text{CH}_3)_2\text{GeH}_2$ , and  $(\text{CH}_3)_3\text{GeH}$ .

The minimum energy path (MEP) is calculated at the UMP2(FULL)/6-31G(d) level by the IRC theory, and the energies of the MEP are refined by the G2MP2//UMP2 method. The classical potential energy,  $V_{\text{MEP}}$ , and the ground-state vibrational adiabatic potential energy,  $V_a^G$ , which are functions of the intrinsic reaction coordinate  $s$ , are important dynamical parameters. The changes of  $V_{\text{MEP}}$  and  $V_a^G$  with the reaction coordinate for the reaction of H with  $\text{GeH}_4$ ,  $\text{CH}_3\text{GeH}_3$ ,  $(\text{CH}_3)_2\text{GeH}_2$ , and  $(\text{CH}_3)_3\text{GeH}$  are shown in Figure 2. It is interesting to note that the change trends of  $V_{\text{MEP}}$  and  $V_a^G$  are similar for the four reactions; this means that they have similar reaction mechanisms. It can be also seen from Figure 2 that the maximum positions of the  $V_{\text{MEP}}$  and  $V_a^G$  energy curves are almost the same at the G2MP2//UMP2 level for each reaction. The zero-point energy, ZPE, which is the difference of  $V_a^G$  and  $V_{\text{MEP}}$ , is almost unchanged as  $s$  varies. This means that the variational effect will be small for the four reactions. To analyze this behavior in greater detail, we show the variation of the generalized normal mode vibrational frequencies of the reaction of H with  $\text{GeH}_4$  along the MEP in Figure 3.

In the negative limit of  $s$ , the frequencies are associated with the reactants, while in the positive limit of  $s$ , the frequencies

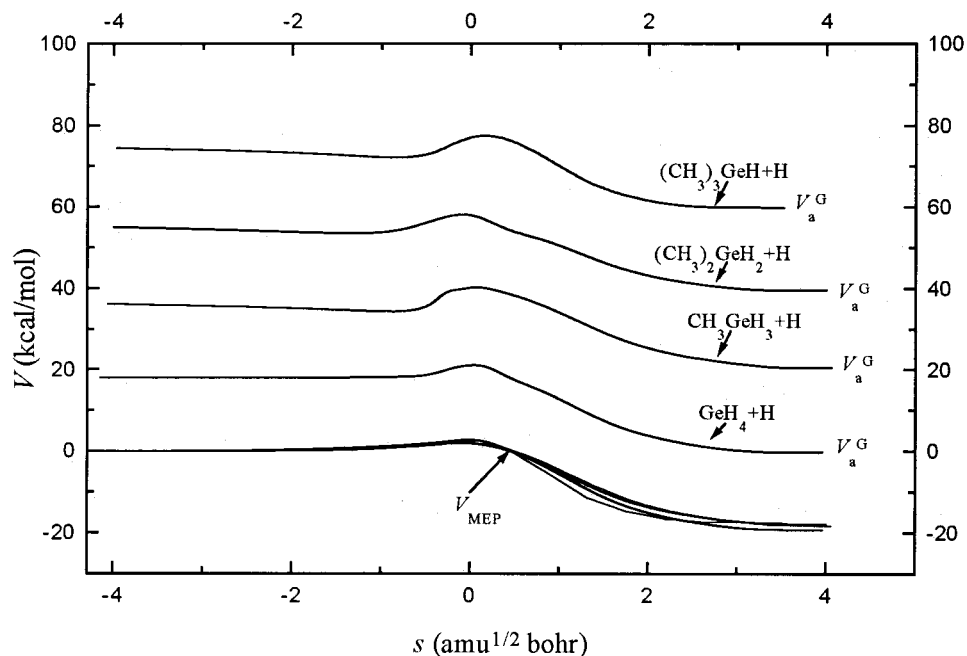


**Figure 2.** The potential energy ( $V_{\text{MEP}}$ ) and vibrationally adiabatic potential energy curves ( $V_a^G$ ) as functions of  $s$  for the reaction of H with  $(\text{CH}_3)_{(4-n)}\text{GeH}_n$  ( $n = 1-4$ ) at the G2MP2//UMP2(FULL)/6-31G(d) level.

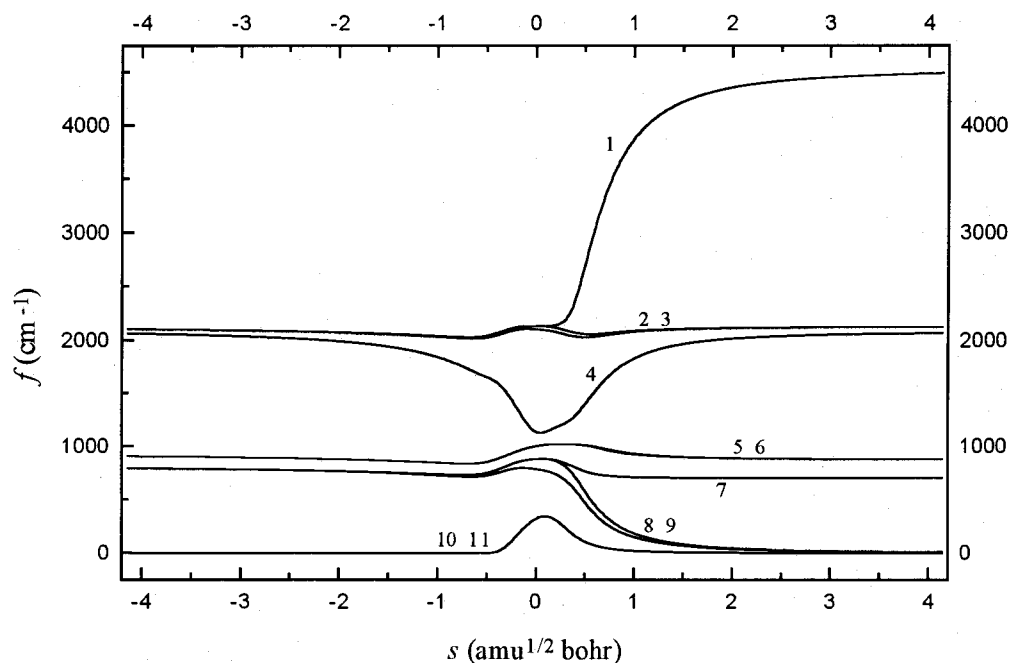


**Figure 3.** Changes of the generalized normal-mode vibrational frequencies as functions of  $s$  at the UMP2(FULL)/6-31(d) level for the reaction of H with  $\text{GeH}_4$ .

are associated with the products. For the sake of clarity, the vibrational frequencies can be divided into three types: spectator modes, transitional modes, and reactive modes. The spectator modes are those that undergo little change and sometimes remain basically unchanged in going from reactants to the transition state. The transitional modes appear along the reaction path as a consequence of the transformation from free rotation or free translations within the reactant or the product limit into real vibrational motions in the global system. Their frequencies tend to zero at the reactant and the product limit and reach their maximum in the saddle-point zone. The reactive modes are those that undergo the largest change in the saddle-point zone, and therefore, they must be related to the breaking/forming bonds. For the reaction of H with  $\text{GeH}_4$ , mode 4, which connects the

frequency of Ge-H stretching vibration of  $\text{GeH}_4$  with the frequency of the H-H stretching vibration of  $\text{H}_2$ , is the reactive mode, modes 10 and 11 are transitional modes, and other modes are spectator modes. From  $s = -0.5$  to  $s = 0.5$   $\text{amu}^{1/2} \text{ b}$ , the reactive modes drop dramatically; this behavior is similar to that found in other hydrogen abstraction reactions.<sup>35-37</sup> A priori, this drop should cause a considerable fall in the zero-point energy near the transition state. But because this kind of drop of the reactive mode is compensated partially by the transitional modes, the zero-point energy shows very little change with the change of the reaction coordinate,  $s$ , and the classical potential energy,  $V_{\text{MEP}}$ , and the ground-state vibrational adiabatic potential energy,  $V_a^G$ , curves are similar in shape. For the same reason,

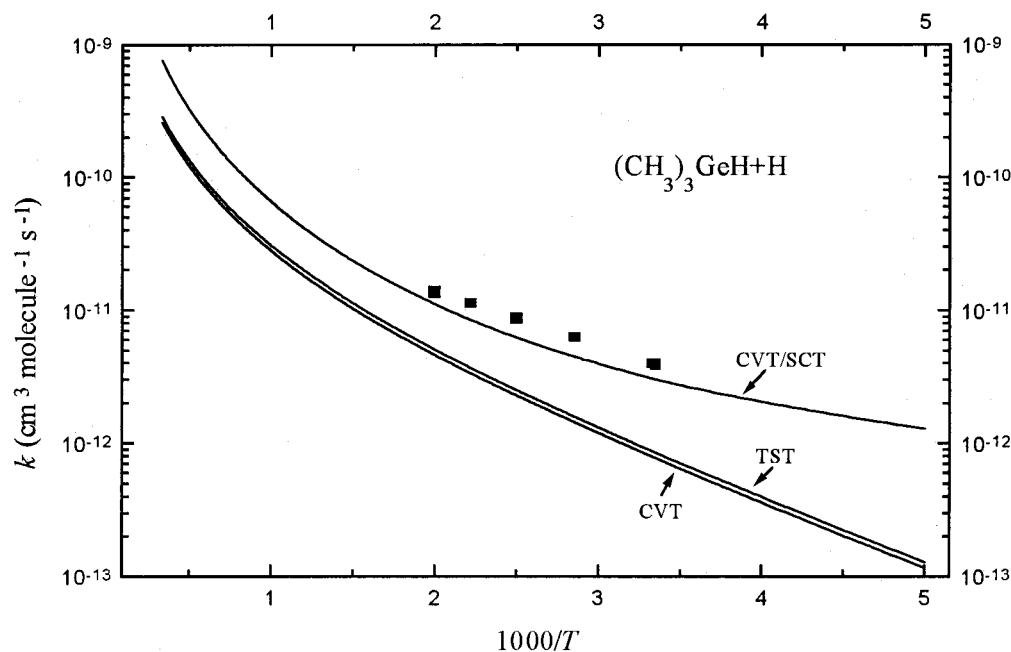


**Figure 4.** Rate constants as a function of the reciprocal of the temperature (K) in the temperature range of 200–3000 K for the reaction of H with  $(\text{CH}_3)_3\text{GeH}$ .

the classical potential energy,  $V_{\text{MEP}}$ , and the ground-state vibrational adiabatic potential energy,  $V_a^G$ , curves are similar in shape for the reactions of H with  $\text{CH}_3\text{GeH}_3$ ,  $(\text{CH}_3)_2\text{GeH}_2$ , and  $(\text{CH}_3)_3\text{GeH}$ .

*b. The Rate Constants.* The canonical variational transition-state theory (CVT) with the small-curvature tunneling correction (SCT), which has been successfully performed for several analogous reactions,<sup>38–40</sup> is an effective method to calculate the rate constants. In this paper, we used this method to calculate the rate constants of the reactions of H with  $\text{GeH}_4$ ,  $\text{CH}_3\text{GeH}_3$ ,  $(\text{CH}_3)_2\text{GeH}_2$ , and  $(\text{CH}_3)_3\text{GeH}$  over a wide temperature range from 200 to 3000 K.

To calculate the rate constants, 30 points are selected near the transition state along the MEP, 15 points in the reactant zone, and 15 points in the product zone. The calculated CVT/SCT rate constants are listed in Table 5 for these four reactions. The experimental values are shown in Table 6 for comparison purposes. It can be seen from Tables 5 and 6 that the calculated rate constants are in excellent agreement with the experimental values. Therefore, the CVT/SCT method is a good choice to calculate accurate rate constants for the title systems.

To compare further the CVT/SCT rate constants with the conventional transition-state theory TST and CVT rate constants, Figure 4 shows the calculated TST, CVT, and CVT/SCT rate constants against the reciprocal of the temperature for the reaction of H with  $(\text{CH}_3)_3\text{GeH}$ . It is seen that the values of TST rate constants and those of CVT rate constants are nearly the same, which enables us to conclude that the variational effect is small for the calculation of the rate constants. This conclusion is in good agreement with the above analysis. The CVT rate constants are much smaller than those of CVT/SCT, especially in the lower-temperature range, which means that the quantum tunneling effect is significant. For example, at 298 K, the CVT rate constant is  $7.73 \times 10^{-13} \text{ cm}^3 \text{ molecule}^{-1} \text{ s}^{-1}$ , while the CVT/SCT rate constant is  $3.01 \times 10^{-12} \text{ cm}^3 \text{ molecule}^{-1} \text{ s}^{-1}$ . The latter is 3.89 times larger than the former. At 1000 K, the CVT rate constant is  $2.78 \times 10^{-11} \text{ cm}^3 \text{ molecule}^{-1} \text{ s}^{-1}$ , while the CVT/SCT rate constant is  $6.52 \times 10^{-11} \text{ cm}^3 \text{ molecule}^{-1} \text{ s}^{-1}$ . The latter is 2.35 times larger than the former. The same

conclusion can be drawn from the reactions of H with  $\text{GeH}_4$ ,  $\text{CH}_3\text{GeH}_3$ , and  $(\text{CH}_3)_2\text{GeH}_2$ .

It is obvious that the CVT/SCT rate constants exhibit typical non-Arrhenius behavior. The CVT/SCT rate constants of the title reactions over the temperature range of 200–3000 K are fitted by a three-parameter formula and given in units of  $\text{cm}^3 \text{ molecule}^{-1} \text{ s}^{-1}$  as follows:

$$k_1 = (2.17 \times 10^{-17})T^{2.16} \exp(-294.2/T) \quad \text{for H with } \text{GeH}_4$$

$$k_2 = (2.21 \times 10^{-17})T^{2.22} \exp(-161.6/T) \quad \text{for H with } \text{CH}_3\text{GeH}_3$$

$$k_3 = (1.96 \times 10^{-17})T^{2.18} \exp(-108.0/T) \quad \text{for H with } (\text{CH}_3)_2\text{GeH}_2$$

$$k_4 = (6.66 \times 10^{-18})T^{2.33} \exp(-60.3/T) \quad \text{for H with } (\text{CH}_3)_3\text{GeH}$$

The effect of the methyl substitution on the Ge–H bond reactivity can be seen by evaluating  $k/n$ , the rate constant corrected for the reaction-path degeneracy, where  $n$  is the number of Ge–H bonds. At 298 K, the  $k/n$  for the reaction of H with  $\text{GeH}_4$  is  $0.47 \times 10^{-12} \text{ cm}^3 \text{ molecule}^{-1} \text{ s}^{-1}$ ; for the reactions of H with  $\text{CH}_3\text{GeH}_3$ ,  $(\text{CH}_3)_2\text{GeH}_2$ , and  $(\text{CH}_3)_3\text{GeH}$ , the values of  $k/n$  are  $1.33 \times 10^{-12}$ ,  $1.59 \times 10^{-12}$ , and  $3.16 \times 10^{-12} \text{ cm}^3 \text{ molecule}^{-1} \text{ s}^{-1}$ , respectively. At 1000 K, the  $k/n$  for the reaction of H with  $\text{GeH}_4$  is  $1.06 \times 10^{-11} \text{ cm}^3 \text{ molecule}^{-1} \text{ s}^{-1}$ ; for the reactions of H with  $\text{CH}_3\text{GeH}_3$ ,  $(\text{CH}_3)_2\text{GeH}_2$ , and  $(\text{CH}_3)_3\text{GeH}$ , the values of  $k/n$  are  $2.86 \times 10^{-11}$ ,  $3.06 \times 10^{-11}$ , and  $6.13 \times 10^{-12} \text{ cm}^3 \text{ molecule}^{-1} \text{ s}^{-1}$ , respectively. It can be seen that the values of  $k/n$  increase with the increase in the methyl substitution from  $\text{GeH}_4$  to  $(\text{CH}_3)_3\text{GeH}$  through  $\text{CH}_3\text{GeH}_3$  and  $(\text{CH}_3)_2\text{GeH}_2$ . This means that the methyl substitution increases the reactivity of the Ge–H bond, which supports the view that the Ge–H bond dissociation energies in  $(\text{CH})_{(4-n)}\text{GeH}_n$  are 3.3–6.9 kcal/mol less than those in  $\text{GeH}_4$  at 0 K.<sup>41</sup>



#### IV. Conclusion

In this paper, we have studied systematically the reactions of H with GeH<sub>4</sub>, CH<sub>3</sub>GeH<sub>3</sub>, (CH<sub>3</sub>)<sub>2</sub>GeH<sub>2</sub>, and (CH<sub>3</sub>)<sub>3</sub>GeH using ab initio methods and the canonical variational transition-state theory (CVT) with the small-curvature tunneling effect. Both the reaction mechanism and the rate constants were reported over the temperature range of 200–3000 K. Several major conclusions can be drawn from this calculation.

(1) The hydrogen abstractions from Ge–H bonds are the sole channel for the reactions of H with (CH<sub>3</sub>)<sub>4-n</sub>GeH<sub>n</sub> ( $n = 1-3$ ).

(2) The four title reactions have similar reaction mechanisms. The transition states involved in these reactions have rather early character.

(3) The calculated potential barrier for the reaction of H with GeH<sub>4</sub> is 2.96 kcal/mol. The potential barriers for the reactions of H with methyl germanes are lower by 0.32–0.75 kcal/mol than that of the reaction of H with GeH<sub>4</sub>.

(4) The calculated CVT/SCT rate constants exhibit typical non-Arrhenius behavior.

(5) The methyl substitution decreases the strength of the Ge–H bond and increases its reactivity.

**Acknowledgment.** The authors thank Professor Donald G. Truhlar for providing the POLYRATE 7.8 program. This work is supported by the Research Fund for the Doctoral Program of Higher Education of China.

#### References and Notes

- Doyle, J. R.; Doughty, D. A.; Gallagher, A. *J. Appl. Phys.* **1991**, *69*, 4169.
- Doyle, J. R.; Doughty, D. A.; Gallagher, A. *J. Appl. Phys.* **1992**, *71*, 4727.
- Fegley, B., Jr.; Prinn, R. G. *Astrophys. J.* **1985**, *299*, 1067.
- Noll, K. S.; Knacke, R. F.; Geballe, T. R.; Tokunaga, A. T. *Icarus* **1988**, *75*, 409.
- Choo, K. Y.; Gaspar, P. P.; Wolf, A. P. *J. Phys. Chem.* **1975**, *79*, 1752.
- Austin, E. R.; Lampe, F. W. *J. Phys. Chem.* **1977**, *81*, 1134.
- Nava, D. F.; Payne, W. A.; Marston, G.; Stief, L. J. *J. Geophys. Res.* **1993**, *98*, 5331.
- Arthur, N. L.; Cooper, I. A. *J. Chem. Soc., Faraday Trans.* **1995**, *91*, 3367.
- Arthur, N. L.; Cooper, I. A.; Miles, L. A. *Int. J. Chem. Kinet.* **1997**, *29* (4), 237.
- Johnston, H. S. *Gas-Phase Reaction Rate Constant*; Ronald: New York, 1965.
- Espinosa-Garcia, J. *J. Chem. Phys.* **1999**, *111* (20), 9330.
- Yu, X.; Li, S.-M.; Sun, C.-C. *J. Phys. Chem. A* **2000**, *104*, 9207.
- Austin, E. R.; Lampe, F. W. *J. Phys. Chem.* **1977**, *81*, 1546.
- Arthur, N. L.; Miles, L. A. *J. Chem. Soc., Faraday Trans.* **1998**, *94* (18), 2741.
- Arthur, N. L.; Miles, L. A. *Chem. Phys. Lett.* **1998**, *295*, 531.
- Doncaster, A. M.; Walsh, R. *J. Phys. Chem.* **1979**, *83*, 578.
- Horie, O.; Taege, R.; Reimann, B.; Arthur, N. L.; Potzinger, P. *J. Phys. Chem.* **1991**, *95*, 4393.
- Ding, L.; Marshall, P. *J. Phys. Chem.* **1992**, *96*, 2197.
- Ding, L.; Marshall, P. *J. Am. Chem. Soc.* **1992**, *114*, 5754.
- Arthur, N. L.; Miles, L. A. *J. Chem. Soc., Faraday Trans.* **1998**, *94* (18), 1077.
- Arthur, N. L.; Miles, L. A. *Chem. Phys. Lett.* **1998**, *282*, 192.
- Frisch, M. J.; Trucks, G. W.; Schlegel, H. B.; Gill, P. M. W.; Johnson, B. G.; Robb, M. A.; Cheeseman, J. R.; Keith, T.; Petersson, G. A.; Montgomery, J. A.; Raghavachari, K.; Al-Laham, M. A.; Zakrzewski, V. G.; Ortiz, J. V.; Foresman, J. B.; Cioslowski, J.; Stefanov, B. B.; Nanayakkara, A.; Challacombe, M.; Peng, C. Y.; Ayala, P. Y.; Chen, W.; Wong, M. W.; Andres, J. L.; Replogle, E. S.; Gomperts, R.; Martin, R. L.; Fox, D. J.; Binkley, J. S.; Defrees, D. J.; Baker, J.; Stewart, J. P.; Head-Gordon, M.; Gonzalez, C.; Pople, J. A. *Gaussian 94*, revision E.1; Gaussian, Inc.: Pittsburgh, PA, 1995.
- Baldrige, K. K.; Gordor, M. S.; Steckler, R.; et al. *J. Phys. Chem.* **1989**, *93*, 5107.
- Gonzalez-Lafont, A.; Truong, T. N.; Truhlar, D. G. *J. Chem. Phys.* **1991**, *95* (12), 8875.
- Garrett, B. C.; Truhlar, D. G. *J. Phys. Chem.* **1979**, *83* (8), 1052.
- Steckler, R.; Chuang, Y. Y.; Fast, P. L.; Corchade, J. C.; Coitino, E. L.; Hu, W. P.; Lynch, G. C.; Nguyen, K.; Jackells, C. F.; Gu, M. Z.; Rossi, I.; Clayton, S.; Melissas, V.; Garrett, B. C.; Isaacson, A. D.; Truhlar, D. G. *POLYRATE Version*; University of Minnesota: Minneapolis, MN, 1997.
- Liu, R.; Francisco, J. S. *J. Phys. Chem. A* **1998**, *102*, 9869.
- Harmony, M. D.; Laurie, V. W.; Kuczkowski, R. L.; Schwendeman, R. H.; Ramsay, D. A.; et al. *J. Phys. Chem. Ref. Data* **1979**, *8* (3), 619.
- Mckean, D. C.; Torto, I.; Mackenzie, M. W.; Morrisson, A. R. *Spectrochim. Acta* **1983**, *39A* (5), 387.
- Imai, Y.; Aida, K. *Bull. Chem. Soc. Jpn.* **1981**, *54*, 3323.
- Griffiths, J. E. *J. Chem. Phys.* **1963**, *38*, 2879.
- Clark, E. A.; Weber, A. *J. Chem. Phys.* **1966**, *45*, 1759.
- Arthur, N. L.; Miles, L. A. *Chem. Phys. Lett.* **1998**, *282*, 192.
- Arthur, N. L.; Potzinger, P.; Reimann, B.; Steenbergen, H.-P. *J. Chem. Soc., Faraday Trans.* **1990**, *86*, 1407.
- Espinosa-Garcia, J.; Corchado, J. C. *J. Phys. Chem.* **1996**, *100*, 16561.
- Corchado, J. C.; Espinosa-Garcia, J. *J. Chem. Phys.* **1997**, *106*, 4013.
- Espinosa-Garcia, J.; Corchado, J. C. *J. Phys. Chem.* **1997**, *101*, 7336.
- Yin, H. M.; Yang, B. H.; Han, K. L.; He, G. Z.; Guo, J. Z.; Liu, C. P.; Gu, Y. S. *Phys. Chem. Chem. Phys.* **2000**, *2*, 5093.
- Yu, X.; Li, S. M.; Xu, Z. F.; Li, Z. S.; Sun, C. C. *Chem. Phys. Lett.* **2000**, *320*, 123.
- Yu, Y. X.; Li, S. M.; Xu, Z. F.; Li, Z. S.; Sun, C. C. *Chem. Phys. Lett.* **1999**, *302*, 281.
- Mckean, D. C. *J. Mol. Struct.* **1984**, *113*, 251.
- Collomon, J. H.; Hirota, E.; Kuchitsu, K.; Lafferty, W. J.; Maki, A. G.; Pote, C. S. *Structure Data of Free Polyatomic Molecules*; Springer-Verlag: Berlin, 1976; Vol. 7.
- Shimanouchi, T. *Tables of Molecular Vibrational Frequencies*; National Standards Reference Data Series; National Bureau of Standards, U.S. Government Printing Office: Washington, DC, 1972; Vol. 39.